Automated Assessment of Tumour Microvascular Architecture *In Vivo*

SVEN BECKER[1,2], SEBASTIAN STRIETH[1,2], MARTIN CANIS[1,2], GERHARD PREISSLER[3] and MARTIN E. EICHHORN[1,3]

[1]*Walter Brendel Centre of Experimental Medicine (WBex),*
[2]*Department of Otorhinolaryngology, Head and Neck Surgery, and*
[3]*Department of Surgery, Campus Grosshadern, Ludwig Maximillians University, 81377 Munich, Germany*

Abstract. *Background: Quantitative analysis of tumour angiogenesis is an indispensable prerequisite for the development of novel antivascular treatment strategies. The aim of this study was to develop an automated analysis technique enabling quantitative assessment of complete tumour vascular networks non-invasively in vivo. Materials and Methods: Experiments were performed in A-Mel-3 implanted in transparent dorsal skinfold chambers of the Syrian Golden hamster. Tumours were imaged in two dimensions by means of a computer controlled scanning-table combined with intravital microscopy. Functional vessel density was automatically quantified online with a digital imaging application package. Results: Data for functional vessel density correlated excellently with data obtained by off-line video-based frame-by-frame analysis ($R_{(S)}$=0.947, r^2=0.959, n=48). Conclusion: This new technique enables automated, quantitative assessment of complete tumour vascular networks and therefore provides a promising tool to characterise changes of the entire tumour vascularity in response to antivascular treatment regimes.*

Angiogenesis, the formation of new blood vessels from the endothelium of the existing vasculature, plays a key role in tumour growth, progression and metastasis (1). The growing vascular tumour network guarantees adequate supply of tumour cells with oxygen and nutrients and provides efficient drainage of metabolites. Quantitative analysis of the tumour microvascular architecture is of great importance for the development of vascular targeting treatment strategies (2) as well as for antiangiogenic approaches (3). However, methods for quantitative analysis of microcirculatory parameters *in vivo* are rare.

Different techniques for imaging tumour microvascularity have been developed, including dynamic contrast-enhanced magnetic resonance imaging (DCE-MRI) (4, 5), microbubble contrast-enhanced sonography (6), as well as intravital microscopy in different chamber-preparations (7) and animal models (8, 9). The strength of *in vivo* microscopy is its ability to provide a direct and continuous approach to visualise and quantify tumour microvasculature (10). Microvascular parameters such as functional microvessel density, blood flow and diameter of the microvessels can be measured but are very heterogeneous in different tumour entities and depend on the location within these tumours. In fast proliferating tumours there is a high proliferation of new blood vessels in the tumour rim in contrast to the tumour centre where, due to changes in the surrounding milieu, an increasing number of tumour cells are necrotic (11, 12). This leads to trial results that are highly examiner-dependent if heterogeneously vascularised regions of the tumour are measured. Reproducibility of results, for example for functional vessel density, therefore is low, if only a small number of regions of interest are investigated. Even if tumours are screened almost completely, the vascular network of the tumour and its complexity can hardly be visualised.

The aim of the present study was to develop an automated analysis technique for the quantitative assessment of entire tumour vascular networks *in vivo*. The approach was validated by correlation of the results with data obtained by *in vivo* fluorescence microscopy and off-line video based analysis.

Materials and Methods

Animal and tumour model. Experiments were carried out using male Syrian golden hamsters of 40-50 g body weight (Charles River, Sulzbach, Germany) in accordance with UKCCCR guidelines (13). The animals were housed in single cages and received tap water and standard laboratory food (ssniff Spezialdiaeten GmbH, Soest, Germany) *ad libitum*. To permit quantitative analysis of microvasculature *in vivo*,

Correspondence to: Dr. Sven Becker, Department of Otorhinolaryngology, Head and Neck Surgery, Ludwig Maximilians University, Marchioninistrasse 15, D-81377 Munich, Germany. Tel: +49 8970950, Fax: +49 8970956889, e-mail: sven.becker@med.uni-muenchen.de

Key Words: Tumour, angiogenesis, functional vessel density, vascular network, fluorescence microscopy.

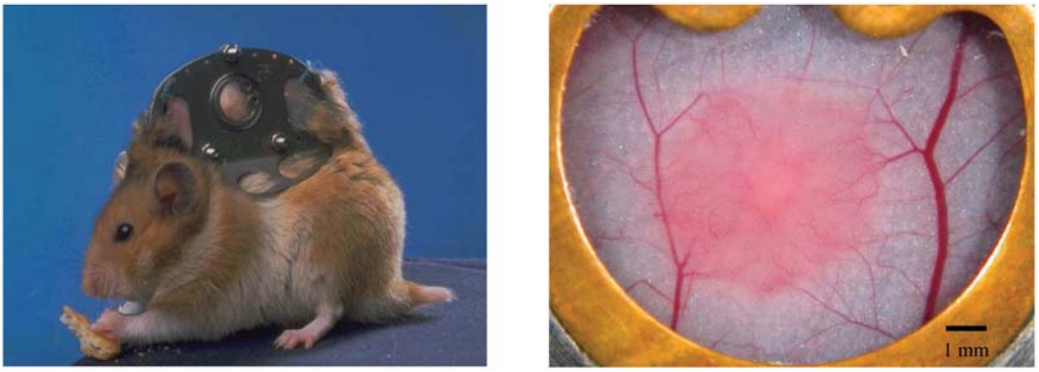

Figure 1. *Dorsal skinfold chamber preparation of the hamster (right). A-Mel-3 tumour at day six after inoculation with 2 μl of dense tumour cell suspension (left).*

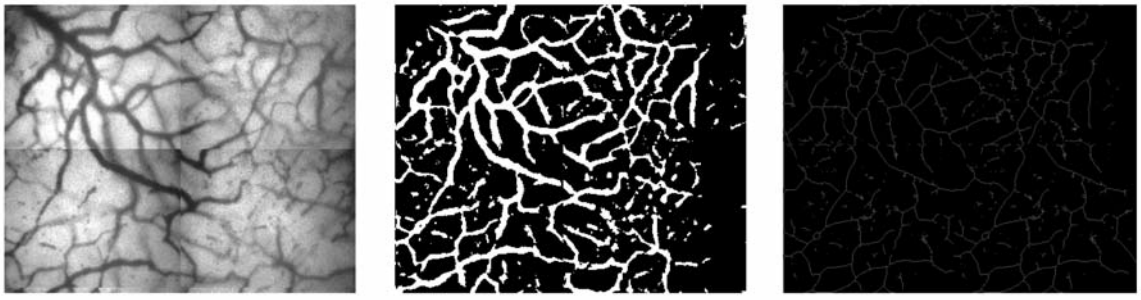

Figure 2. *Four regions of interest acquired in blue light trans-illumination technique (left), after transformation into binary images (middle) and after using the vessel thinning procedure (right).*

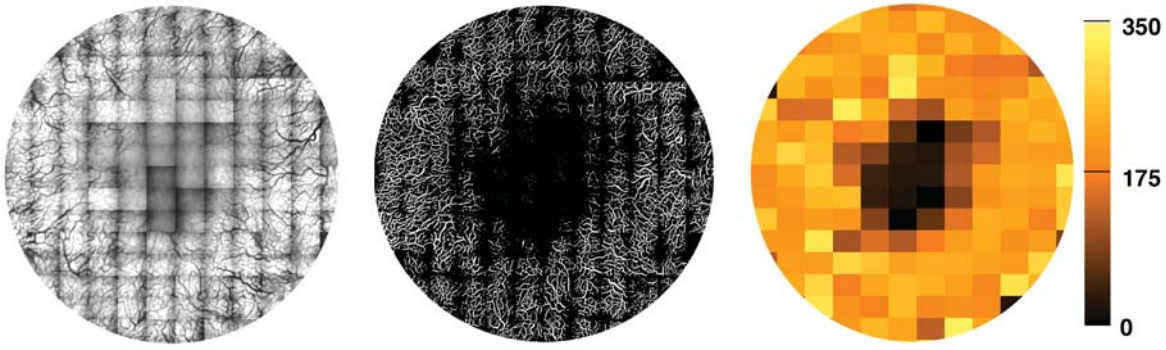

Figure 3. *Complete tumour vasculature (tumour #1) using the blue light transillumination technique (left) and after transformation into a binary image (middle). The false colour rendering of the functional vessel density (fvd) map (right) shows the difference between the fast proliferating tumour rim and necrotic areas in the tumour centre (fvd is expressed in cm^{-1}).*

a dorsal skinfold chamber, consisting of two symmetric titanium frames, was surgically implanted into the dorsal skin of the animals as described previously (14, 15). After a recovery period of 24 h from anaesthesia and microsurgery, chamber preparations were inoculated with 2 μl of dense tumour cell suspension (~2×10^5 cells) of the amelanotic melanoma of the hamster A-Mel-3 (16) (Figure 1). For the administration of flouroscence markers, permanently indwelling fine polyethylene catheters (PE10; inner diameter, 0.28 mm) were implanted into the right jugular vein. All surgical procedures were performed under anaesthesia with ketamine (100 mg/kg body weight *i.p.*, Ketavet®; Parke-Davis, Berlin, Germany) and xylazine (10 mg/kg body weight *i.p.*, Rompun®; Bayer, Leverkusen, Germany).

In vivo microscopy. For *in vivo* microscopy, the awake and chamber-bearing hamster was immobilised in a Perspex tube on a specially designed stage (Effenberger, Munich, Germany) under a modified

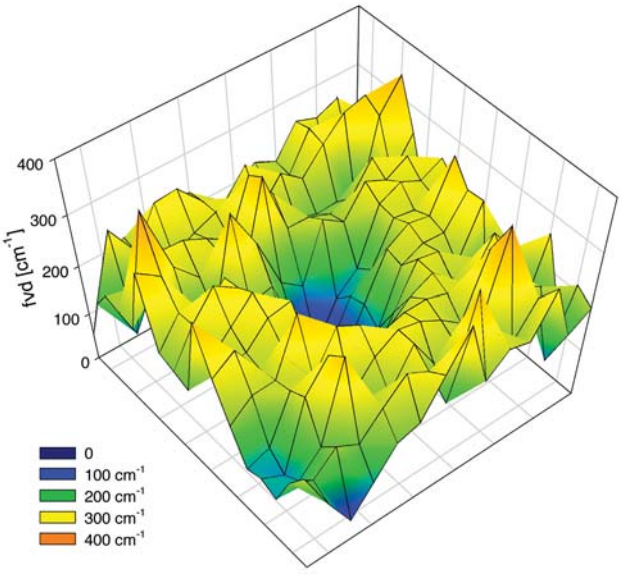

Figure 4. *3D-mesh graph of functional vessel density (fvd) in tumour #1. Data from 238 ROIs (14 in x direction, 17 in y direction) were used to create the graph.*

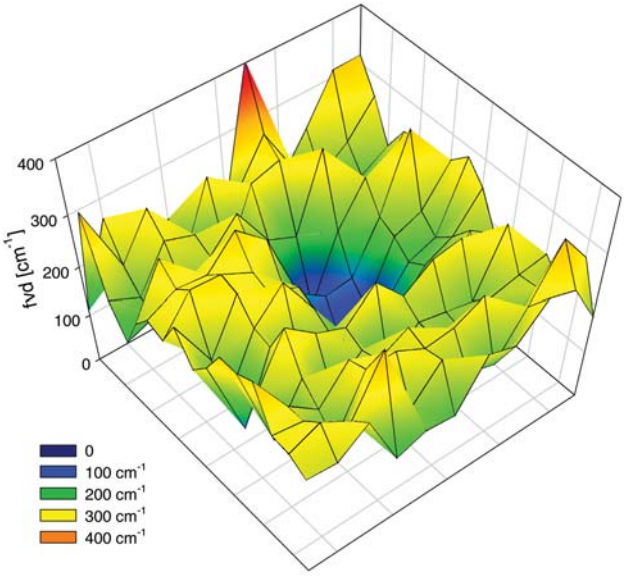

Figure 5. *3D-mesh-graph of functional vessel density (fvd) in tumour #2. Data from 176 ROIs (11 in x direction, 16 in y direction) were used to create the graph.*

Leitz microscope (Orthoplan; Leitz, Munich, Germany). After setting the starting point and the number of images that should be taken in x and y directions, the tumour was scanned in two dimensions and imaged by means of a computer controlled scanning table. Images had a 10% overlap in x and y directions. Blue light transillumination technique with a magnification of 630-fold and automated focusing was used to assure good quality of the acquired images.

Image analysis. Analysis of the acquired images was performed with a digital imaging application package (KS400, Zeiss, Germany) on a personal computer (Scenic, Siemens Fujitsu, Munich, Germany). The algorithm for the calculation of functional vessel density was programmed using the KS400 macro editor function.

To minimise the loss of quality due to irregular illumination and inhomogeneous sensitivity of the camera sensors, a shading correction procedure was used (shadcorr). The best correction in terms of maximal contrast of the images could be reached with a multiplicative correction (Appendix). In the algorithm, the acquired images had to be transferred into binary images for further processing (Figure 2). This was achieved by a multiple step procedure. In the first step, each pixel of the image was scaled along a grayscale between 0 and 255 (normalize). To amplify the contrast between the light gray background and the darker vessels, the grayscale values of each pixel in the image were multiplied with themselves (multiply) in the second step. Therefore, pixels with low grayscale values such as those in the background stayed low, while pixels with greater values such as those within a vessel were intensified. In the next step, a smooth-function was used to reduce maxima and to abrade sharp edges (median). In the fourth step, each pixel of each image was inverted; for example, black was inverted to white and light gray was inverted to dark gray (binnot). The final step was a gray value segmentation to result in a binary image (disdyn). The code for the multiple step procedure is given in the Appendix. Finally the vessels, now white in the binary images, were reduced to single lines along their smallest diameter by a thinning procedure (binthinning) developed by Arcelli *et al*. (17) (Appendix).

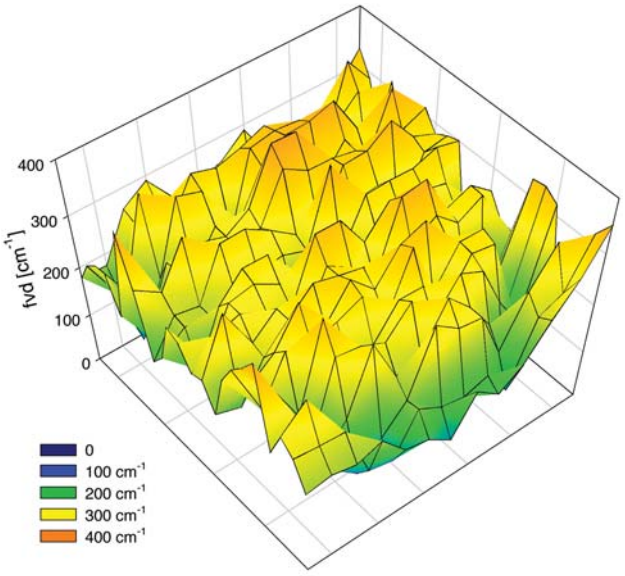

Figure 6. *3D-mesh-graph of functional vessel density (fvd) in tumour #3. Data from 286 ROIs (13 in x direction, 22 in y direction) were used to create the graph. In contrast to tumour #1 and #2 there was no difference between tumour rim and centre.*

The length of all lines/vessels within a region of interest (ROI) was calculated and divided through the area of the ROI. The result was saved on the computer as a functional vessel density map together with the ID number of the ROI. The whole procedure was performed online by means of the aforementioned self-written

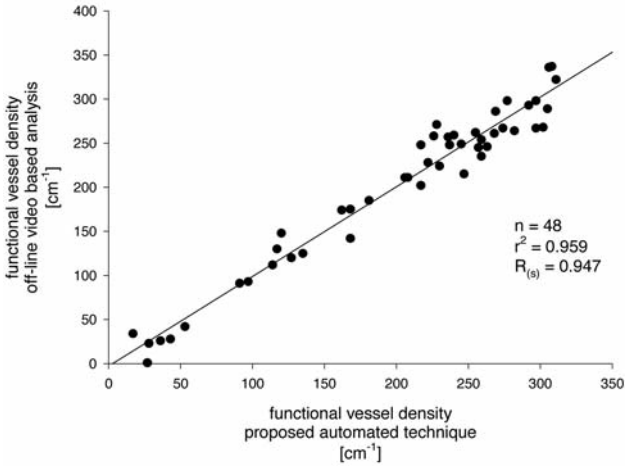

Figure 7. *Linear regression of 48 ROIs measured by the off-line video based analysis and by the proposed automated technique.*

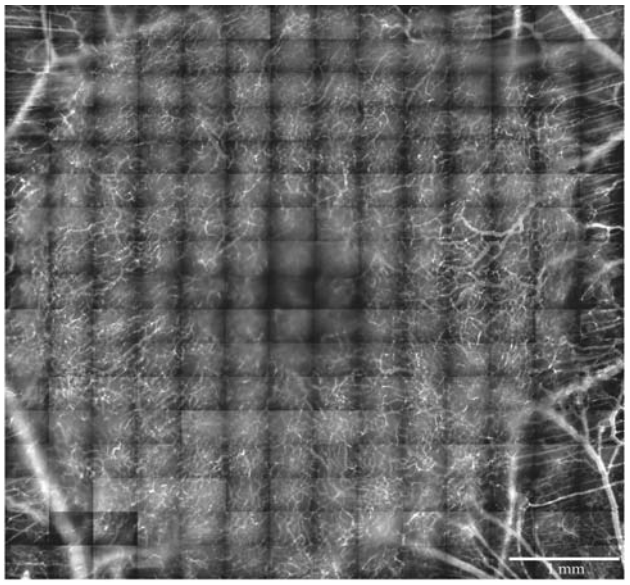

Figure 8. *Complete tumour vascular network (tumour #1) with surrounding normal tissue using fluorescence microscopy to visualise the functional vascularity of the tumour.*

algorithm. To visualise differences in functional vessel density among different areas of the tumour, false colour rendering and 3D-mesh-graphs were used (Figures 3, 4, 5 and 6).

Fluorescence microscopy. For the validation of this new technique, the data were correlated with the results acquired by *in vivo* fluorescence microscopy and off-line video analysis. For this purpose, FITC-labelled dextran (MW 500000; 0.05-0.1 ml of a 5% solution in 0.9% NaCl; Sigma, Deisenhofen, Germany) was injected intravenously to visualise tumour microcirculation. Selective observation of FITC-labelled plasma was carried out using epi-illumination with a 100 W mercury lamp attached to a Leitz Ploemopak illuminator with a Leitz I2/3 filter block (excitation wavelength: 450-490 nm, emission wavelength ≥515 nm). *In vivo* fluorescence microscopy was performed immediately after the scanning procedure of the tumour. The scanning table was set back to randomly selected ROIs where images were acquired by a SIT video camera (C2400-08; Hamamatsu, Herrsching, Germany) and recorded on a S-VHS video tape.

Off-line analysis of the S-VHS video tapes was performed by an image analysis system (Cap Image; Zeintl, Heidelberg, Germany) (18). This system allowed the measurement of functional vessel density as a parameter for angiogenic activity (19).

Study protocol. For data acquisition, three animals with constant growing tumours and chamber preparations without irritations were used (20). Twenty-four hours after surgical chamber preparation, tumour cells were implanted and jugular vein catheters were inserted. The scanning procedure was performed on day 6 after tumour cell inoculation. Fluorescent markers were injected 30 min before measurement.

Results

The three tumours were completely scanned with up to 286 ROIs (13×22 ROIs in x and y directions) depending on tumour size. After cutting off the normal tissue vasculature, the whole tumour vascular network was visualised in blue-light transillumination for further processing (Figure 3, left). By running the new automated algorithm, binary images of the entire tumour vasculature were created. These images were used for the quantification of functional vessel density (fvd) in each ROI (Figure 3, middle). To visualise differences in fvd in different parts of the tumour, false colour rendering (Figure 3, right) and 3D-mesh-graphs were used (Figure 4, 5 and 6).

Differences in fvd between the fast proliferating tumour rim and the tumour centre were detected in two of the three tumours. Tumour #1 had an fvd of 217.1 cm^{-1} in the tumour rim and an fvd of 81.0 cm^{-1} in the tumour centre (Figure 4). The analysis of tumour #2 resulted in an fvd of 215.1 cm^{-1} in the tumour rim and an fvd of 80.1 cm^{-1} in the tumour centre (Figure 5). In tumour #3 it was not possible to differentiate between the rim and the centre; the fvd of the whole tumour was 252.6 cm^{-1} (Figure 6).

To validate this new approach, 48 randomly selected ROIs out of the three tumours were also examined by fluorescence microscopy and off-line video based frame-by-frame analysis. Correlation of data of both techniques revealed a Spearman's correlation coefficient of $R_{(s)}$=0.947 (r^2=0.959, n=48) for functional vessel density (Figure 7).

The scanning procedure of the entire vascular network was also used in combination with fluorescence microscopy to get reliable data of the actually perfused parts in the tumour (Figure 8).

Discussion

Intravital microscopy is one of the leading techniques to study tumour microcirculation (10). However, it has not yet been possible to visualise the complexity of whole tumour microvascular networks. Therefore in this study, an examiner-independent automated procedure was developed to measure tumour vascularity in terms of fvd. The strength of this new technique is its ability to visualise and analyse the complex microvascular structure of entire tumours without examiner-dependent bias. The results correlated well with data obtained by fluorescence microscopy and off-line video based frame-by-frame analysis. Previous studies showed comparable but slightly higher results for fvd in untreated A-Mel-3 tumours (21). This overestimation may be due to the fact that only a small number of ROIs was measured in that study (20).

This new technique using blue-light transillumination microscopy, however, failed to distinguish between perfused and non-perfused microvessels because it was not possible to set a threshold for separating one against the other. Nevertheless, measurement of fvd with this new approach and fluorescence microscopy showed comparable results in the A-Mel-3 tumour. This indicates a high functional efficacy of the newly formed blood vessels.

Attempts to combine the newly developed algorithm with fluorescence microscopy for a single measurement of perfused vessels failed because the contrast between FITC-labelled plasma and the extravascular background was too low to reach a sufficient transformation into binary images. However, the generation of clear binary images is a prerequisite for a correct calculation of vessel density. To reach this goal a precise illumination and shading correction of the whole ROI especially at the edges is necessary when acquiring the initial images. This may be difficult in long-term observations when the tumour is growing in three dimensions and transillumination decreases. A 10% overlap of the images in x and y directions can reduce this problem.

In comparison to other techniques for the measurement of tumour microcirculation such as DCE-MRI and microbubble contrast-enhanced sonography, the present technique gives no information about the functionality of the tumour vessels. Hyperperfusion or stasis in different parts of the tumour cannot be detected as well as the formation of thrombosis within the vessels. In contrast, DCE-MRI can be used to quantify tumour perfusion and tumour vessel permeability and to characterise the intra- and extravascular compartments. Unfortunately, there is a number of different tracer kinetic models with a variety of microvascular parameters, making the comparability among different DCE-MRI studies very difficult. Furthermore, there are no standardised measurement protocols to compare studies from different institutions (22, 23). Similar problems occur when using microbubble contrast-enhanced sonography. Despite its low cost, its availability and its first promising results in monitoring antivascular therapy there is also a lack in standardisation so far (24, 25).

The results of the present study demonstrated the heterogeneity of functional vessel density between the fast proliferating tumour rim and the increasingly necrotic tumour centre which could be seen in two of the three tumours. These findings were due to the decreasing nutrient and oxygen supply to the tumour centre normally seen around day 4 to 5 after tumour cell inoculation (14). Tumour #3 was smaller in diameter and therefore could have had a better supply of oxygen and nutrients for the central tumour parts where no necrotic areas were observed.

Graphical illustration by 3D meshes and false colour rendering enabled the visualisation of functional vessel density within the tumours and can be used to characterize changes of the entire tumour vascular network in response to antivascular treatment regimes.

The new algorithm is not only an application for the skinfold chamber in the hamster, but can also be used for other preparations and tumour models; for example in the cranial window preparation of rats or mice (26). The only limitation is that the acquired images must have enough contrast between the vessels and the background to achieve a good transformation into binary images.

In this study, an automated examiner-independent technique was developed for the assessment of tumour microvasculature. Further studies will focus on the improvement of this imaging technique to make other microcirculatory parameters such as vessel diameter and red blood cell velocity accessible for automated imaging and quantification algorithms.

Appendix - Processing procedures in KS400 environment

Shading correction
imgdelete “*”
imgload “ROI1”,1
imgload “shading_correction.img”,4
shadcorr 1,4,2,2,0

Multistep image transfer
normalize 1,2,0
multiply 2,2,3,200
median 3,4,7
binnot 4,5
disdyn 5,6,65,-20,1

Vessel thinning
binthinning 1,2,1,0

References

1 Folkman J: Angiogenesis in cancer, vascular, rheumatoid and other disease. Nat Med *1*: 27-31, 1995.

2 Denekamp J: Vascular endothelium as the vulnerable element in tumours. Acta Radiol Oncol *23*: 217-225, 1984.

3 Jain RK, Schlenger K, Hockel M and Yuan F: Quantitative angiogenesis assays: progress and problems. Nat Med *3*: 1203-1208, 1997.

4 Brasch RC, Li KC, Husband JE, Keogan MT, Neeman M, Padhani AR, Shames D and Turetschek K: *In vivo* monitoring of tumor angiogenesis with MR imaging. Acad Radiol *7*: 812-823, 2000.

5 Eichhorn ME, Becker S, Strieth S, Werner A, Sauer B, Teifel M, Ruhstorfer H, Michaelis U, Griebel J, Brix G, Jauch KW and Dellian M: Paclitaxel encapsulated in cationic lipid complexes (MBT-0206) impairs functional tumor vascular properties as detected by dynamic contrast enhanced magnetic resonance imaging. Cancer Biol Ther *5*: 89-96, 2006.

6 Strohmeyer D, Frauscher F, Klauser A, Recheis W, Eibl G, Horninger W, Steiner H, Volgger H and Bartsch G: Contrast-enhanced transrectal color doppler ultrasonography (TRCDUS) for assessment of angiogenesis in prostate cancer. Anticancer Res *21*: 2907-2913, 2001.

7 Endrich B, Asaishi K, Götz A and Messmer K: Technical report – a new chamber technique for microvascular studies in unanesthetized hamsters. Res Exp Med (Berl) *177*: 125-134, 1980.

8 Menger MD, Marzi I and Messmer K: *In vivo* fluorescence microscopy for quantitative analysis of the hepatic microcirculation in hamsters and rats. Eur Surg Res *23*: 158-169, 1991.

9 ALGIRE GH and MERWIN RM: vascular patterns in tissues and grafts within transparent chambers in mice. Angiology *6*: 311-318, 1955.

10 Vajkoczy P, Ullrich A and Menger MD: Intravital fluorescence videomicroscopy to study tumor angiogenesis and microcirculation. Neoplasia *2*: 53-61, 2000.

11 Vajkoczy P, Schilling L, Ullrich A, Schmiedek P and Menger MD: Characterization of angiogenesis and microcirculation of high-grade glioma: an intravital multifluorescence microscopic approach in the athymic nude mouse. J Cereb Blood Flow Metab *18*: 510-520, 1998.

12 Vajkoczy P, Menger MD, Vollmar B, Schilling L, Schmiedek P, Hirth KP, Ullrich A and Fong TA: Inhibition of tumor growth, angiogenesis, and microcirculation by the novel Flk-1 inhibitor SU5416 as assessed by intravital multi-fluorescence video-microscopy. Neoplasia *1*: 31-41, 1999.

13 United Kingdom Co-ordinating Committee on Cancer Research (UKCCCR) Guidelines for the Welfare of Animals in Experimental Neoplasia (Second Edition). Br J Cancer *77*: 1-10, 1998.

14 Asaishi K, Endrich B, Gotz A and Messmer K: Quantitative analysis of microvascular structure and function in the amelanotic melanoma A-Mel-3. Cancer Res *41*: 1898-1904, 1981.

15 Endrich B, Hammersen F, Gotz A and Messmer K: Microcirculatory blood flow, capillary morphology and local oxygen pressure of the hamster amelanotic melanoma A-Mel-3. J Natl Cancer Inst *68*: 475-485, 1982.

16 Fortner JG, Mahy AG and Schrodt GR: Transplantable tumors of the Syrian (golden) hamster. I. Tumors of the alimentary tract, endocrine glands and melanomas. Cancer Res *21(6)Pt 2*: 161-198, 1961.

17 Arcelli C, Cordella L and Levialdi S: Parallel thinning of binary pictures. Electronic Lett *11*: 148-149, 1975.

18 Zeintl H, Sack FU, Intaglietta M and Messmer K: Computer-assisted leukocyte adhesion measurement in intravital microscopy. Int J Microcirc Clin Exp *8*: 293-302, 1989.

19 Dellian M, Witwer BP, Salehi HA, Yuan F and Jain RK: Quantitation and physiological characterization of angiogenic vessels in mice: effect of basic fibroblast growth factor, vascular endothelial growth factor/vascular permeability factor, and host microenvironment. Am J Pathol *149*: 59-71, 1996.

20 Steinbauer M, Harris AG and Messmer K: Effects of dextran on microvascular ischemia-reperfusion injury in striated muscle. Am J Physiol *272*: H1710-H1716, 1997.

21 Strieth S, Eichhorn ME, Sauer B, Schulze B, Teifel M, Michaelis U and Dellian M: Neovascular targeting chemotherapy: encapsulation of paclitaxel in cationic liposomes impairs functional tumor microvasculature. Int J Cancer *110*: 117-124, 2004.

22 Barrett T, Brechbiel M, Bernardo M and Choyke PL: MRI of tumor angiogenesis. J Magn Reson Imaging 26: 235-249, 2007.

23 Charnley N, Donaldson S and Price P: Imaging angiogenesis. Methods Mol Biol *467*: 25-51, 2009.

24 Korpanty G, Carbon JG, Grayburn PA, Fleming JB and Brekken RA: Monitoring response to anticancer therapy by targeting microbubbles to tumor vasculature. Clin Cancer Res *13*: 323-330, 2007.

25 Lavisse S, Lejeune P, Rouffiac V, Elie N, Bribes E, Demers B, Vrignaud P, Bissery MC, Brule A, Koscielny S, Peronneau P and Lassau N: Early quantitative evaluation of a tumor vasculature disruptive agent AVE8062 using dynamic contrast-enhanced ultrasonography. Invest Radiol *43*: 100-111, 2008.

26 Yuan F, Salehi HA, Boucher Y, Vasthare US, Tuma RF and Jain RK: Vascular permeability and microcirculation of gliomas and mammary carcinomas transplanted in rat and mouse cranial windows. Cancer Res *54*: 4564-4568, 1994.

Received March 30, 2010
Revised May 19, 2010
Accepted May 26, 2010